Ultrasonics 116 (2021) 106521

Contents lists available at ScienceDirect

Ultrasonics

journal homepage: www.elsevier.com/locate/ultras

Ultrasonic fatigue testing of concrete

Michael Fitzka [a], Ulrike Karr [a], Maximilian Granzner [b], Tomáš Melichar [c], Martin Rödhammer [d], Alfred Strauss [b], Herwig Mayer [a,*]

[a] Institute of Physics and Materials Science, University of Natural Resources and Life Sciences, Vienna, Austria
[b] Institute of Structural Engineering, University of Natural Resources and Life Sciences, Vienna, Austria
[c] Institute of Technology of Building Materials and Components, Brno University of Technology, Brno, Czech Republic
[d] AMiP Industrial Engineering GmbH, Gießhübl, Austria

ARTICLE INFO

Keywords:
Concrete
Very high cycle fatigue
Ultrasonic fatigue
Cyclic compression testing
Fatigue damage monitoring
Computed tomography

ABSTRACT

Cyclic compression fatigue properties of concrete are studied with the ultrasonic fatigue testing method with cycling frequency 19 kHz and are compared to servo-hydraulic tests performed at 60 Hz. Ultrasonic testing was found applicable for rapid generation of very high cycle fatigue (VHCF) data of concrete. Fatigue cracks can be initiated, however specimens do not rupture, since cyclic stresses decrease with increase of compliance in displacement controlled ultrasonic tests. Observation of resonance frequency, analysis of higher order harmonics of vibration, and computed tomography of specimens are successful methods to analyse fatigue damage. Calorimetric evaluations can be used to calculate the cyclic irreversible strain, which is about 1% of the elastic strain in the ultrasonic VHCF test.

1. Introduction

Concrete is increasingly used in structures, where cyclically varying loads besides static stresses are present. Numerous repetitive loads are imposed on concrete structures e.g. by engine vibrations applying forces on fundaments, gravitational and acceleration forces of motor vehicles stressing pavements and bridges, forces caused by gusts of wind or periodic impact forces of sea waves. Cyclic loading can lead to fatigue damage in concrete, even though all load cycles are well below its static strength [1–17].

The number of load cycles acting on concrete structures can be very high. Concrete bridges [5], offshore structures [6], and foundations of wind turbines [8] can accumulate more than 10^8 load cycles during their lifetimes. Understanding of the fatigue properties of concrete in the very high cycle fatigue (VHCF) regime (i.e. above 10^7 cycles) is therefore necessary for safe design of components.

Fatigue properties of concrete are characterized in fatigue tests, where samples are stressed with a cyclically varying compression force until fracture. The fatigue lifetime is determined as a function of the relative maximum stress level, i.e. the maximum compression stress of a load cycle divided by the static compression strength of the material for the same sample geometry. Servo-hydraulic equipment is mostly used for fatigue testing. Testing of concrete is typically performed at cycling frequencies below 10 Hz due to the limitations of servo-hydraulic testing equipment. Testing in the VHCF regime, however, becomes very time consuming with this testing technique. Loading one single specimen with 10^8 cycles would require up to several months, and several specimens must be tested for a statistically reliable set of data. This makes plausible, why fatigue data of concrete published in literature is mostly limited to numbers of cycles below approximately 10^7 [16], and fatigue limits are typically defined on the basis of a limiting lifetime of 2×10^6 cycles [12]. Fatigue properties above 10^8 cycles are theoretically predicted [18], since experimental verification using standard testing techniques is hardly feasible.

Testing times can be drastically shortened using the ultrasonic fatigue testing method. In concrete research, ultrasonic measurements usually refer to non-destructive ultrasonic sounding techniques, especially for monitoring the concrete curing process using wave velocity measurements [19,20]. Ultrasonic pulse velocity measurements are also used to monitor stiffness degradation during fatigue loading [14]. Ultrasonic fatigue testing, however, refers to accelerated fatigue testing of materials using a high frequency testing setup. This method works at cycling frequencies close to 20 kHz and is therefore in principle most appropriate for fatigue testing in the VHCF regime. Ultrasonic fatigue testing is being used since half a century, to study the fatigue properties of metallic materials, mainly under push–pull loading conditions

* Corresponding author.
E-mail address: herwig.mayer@boku.ac.at (H. Mayer).

https://doi.org/10.1016/j.ultras.2021.106521
Received 30 October 2020; Received in revised form 6 July 2021; Accepted 6 July 2021
Available online 10 July 2021

[21,22]. Several new testing capabilities have been developed over the years that extended the possibilities of this technique, including testing with superimposed mean loads to the high frequency vibration, testing under multiaxial or torsional loading conditions, in different environments, at different temperatures etc. [23]. A recent survey of technical details, experimental capabilities and interesting studies performed with ultrasonic fatigue testing equipment is available in [24].

Compared with the cycling frequencies in the range between 1 Hz and 10 Hz used in servo-hydraulic tests of concrete, samples are loaded with more than a factor 1000 higher cycling frequency in ultrasonic tests. This leads to the question, if fatigue behaviour studied at very high strain rates are of practical relevance for actual components being typically stressed at decades lower cycling frequencies. In literature, increasing fatigue lifetimes of concrete with increasing cycling frequency are described [1–3,10,11,13,15]. An explanation for the increased lifetimes at the higher cycling frequency is the increase of strength of concrete with increasing strain rates [25]. Strain rates are proportional to the cycling frequency for sinusoidal loading. Therefore, the strain rates in ultrasonic fatigue tests are equally more than a factor 1000 higher than in servo-hydraulic tests, and frequency effects must be considered.

Besides the drastically increased cycling frequency, the ultrasonic fatigue testing procedure is different from conventional force controlled fatigue testing e.g. with servo-hydraulic equipment in several other respects. Specimens are stimulated to high frequency resonance vibrations rather than being stressed by external forces. The vibration amplitude of one end of the specimen rather than the applied force is used to control loading, since cyclic forces or stresses cannot be measured directly in the ultrasonic fatigue test. Strain gauges are used to measure cyclic straining of the sample, and stress amplitudes are calculated with the stiffness of the material.

The design of the specimens is constrained in ultrasonic tests, since the specimen shape must fulfil the resonance criterion. This is an important difference to conventional fatigue tests, where the sample geometry can be chosen more freely. The length of concrete samples is the resonance length at ultrasonic frequency. The diameter of the specimen is restricted due to maximum power of the ultrasonic equipment. This leads to a significantly smaller testing volume compared with concrete samples used in conventional fatigue tests. Due to the size effect [26], longer lifetimes for the smaller specimens must be expected. Also, the heat generated by ultrasonic frequency cycling must be considered. Continuous loading at ultrasonic frequency would lead to an undesirable increase of specimen temperature and invalid test results. Intermitted rather than continuous loading must be applied, the specimens must be air-cooled and temperature must be monitored to guarantee that the temperature of the sample remains below an allowable maximum.

In a previous work an experimental setup for ultrasonic fatigue testing of concrete under cyclic compression loading has been developed [27]. Two types of concrete have been cycled with maximum number of load cycles of 10^9. The evolution of fatigue cracks has been documented via Computed Tomography (CT) investigations of the virgin specimen and after ultrasonic fatigue cycling. The study showed that cyclic compression fatigue testing of concrete with the ultrasonic fatigue testing method is in principle possible [27]. However, the ultrasonic fatigue tests could not be compared to conventional fatigue tests. It is therefore uncertain, how fatigue properties measured with the ultrasonic technique comply with data obtained with conventional technique.

The present work serves to compare testing capabilities and peculiarities and the obtained fatigue damage in concrete after ultrasonic and servo-hydraulic testing. The endurance limit is determined at ultrasonic frequency in displacement controlled tests and at 60 Hz in stress controlled tests. Cylindrical concrete samples with the same (relatively small) stressed volume are used in both tests to avoid size effects on the measured results. Disintegration of the specimen is the trivial failure criterion in servo-hydraulic fatigue tests. In contrast, ultrasonic loading may lead to the formation of fatigue cracks but it is still impossible to fully fracture a specimen [27]. Criteria for failure based on the vibration properties of the specimen are used as an indirect measure for fatigue damage and failure. Comparing CT reconstructions of the virgin specimen and after ultrasonic cycling serves to observe possibly formed fatigue cracks in concrete.

2. Material and method

2.1. Material

The investigated self-compacting concrete with an intended compressive strength around 120 MPa was cast in blocks of 150 mm edge length. The cubes were kept at 20 °C ± 2 °C and RH = 65 % ± 5 % for 28 days. The basic material and mechanical properties are given in Table 1.

Specimens for ultrasonic and servo-hydraulic fatigue testing were obtained by extracting drill cores with a diameter of 21 mm from cast cubes of 150 mm edge length. The cylinders were cut to length and the surfaces subsequently polished.

A compressive strength of σ_{dB} = (133 ± 18) MPa was determined from compressing cylindrical specimens with a diameter of 21 mm and a length of 35 mm. The compressive modulus E was determined by measuring the strains with two strain gauges with gauge length 20 mm on specimens with a diameter of 21 mm and a length of 120 mm, for compressive stresses between 7 MPa and 16 MPa.

2.2. Testing procedure

2.2.1. Ultrasonic fatigue testing

The ultrasonic fatigue testing technique is based on stimulating specimens to resonance vibrations at ultrasonic frequency. The employed ultrasonic equipment was originally developed for high precision fatigue testing of metallic samples [24], for which it is typically used. The testing technique has been adapted for testing concrete specimens under cyclic (compression) loading with superimposed compression mean loads. The principle of the ultrasonic fatigue testing method is illustrated in Fig. 1.

The ultrasonic load train consists of an ultrasonic converter, a magnifying horn, the specimen, an extension rod, and mounting parts to introduce compressive forces between two vibration nodes (“Mounting 1” and “Mounting 2”). The ultrasonic converter is driven by a sinusoidal voltage signal at the exact resonance frequency of the load train and generates longitudinal push–pull vibrations, injecting the sound wave into the top end of the load train. All individual components (including the specimen) are designed to vibrate in resonance close to the resonance frequency of the ultrasonic converter (approx. 19 kHz for the present setup). Since the excitation frequency is kept at the resonance frequency, a standing wave is established where both ends of each component vibrate in opposite directions with displacement nodes (and hence maximum strain) in their respective centres.

The vibration movement is observed with a vibration gauge close to the top end of the concrete specimen (i.e. at an antinode) and is regulated to a pre-selected amplitude. In this way, the strain in the centre of the specimen is determined, since strain in the centre of the specimen and vibration amplitude at the antinode are proportional. Closed-loop control guarantees ± 1 % agreement between pre-selected and actual amplitude. Additionally, the excitation signal generated by the ultrasonic generator is controlled in a second closed-loop control to exactly coincide with the resonance frequency of the system within ± 1 Hz.

For the present tests, the ultrasonic load train has been inserted into a hydraulic load frame for superimposing compression mean loads (Fig. 2).

Specimen surface temperature is observed with an infrared thermometer. Rather than being cycled continuously, specimens are loaded

Table 1
Material properties of the investigated concrete formulation.

Largest grain ⌀	w/c factor	Aggregate	Cement	Mass density ρ	Compressive modulus E	Compressive strength σ_{dB}
16 mm	0.39	Quartzitic	CEM I 52.5 R	2.40 g/cm^3	(51.9 ± 2.2) GPa	(133 ± 18) MPa

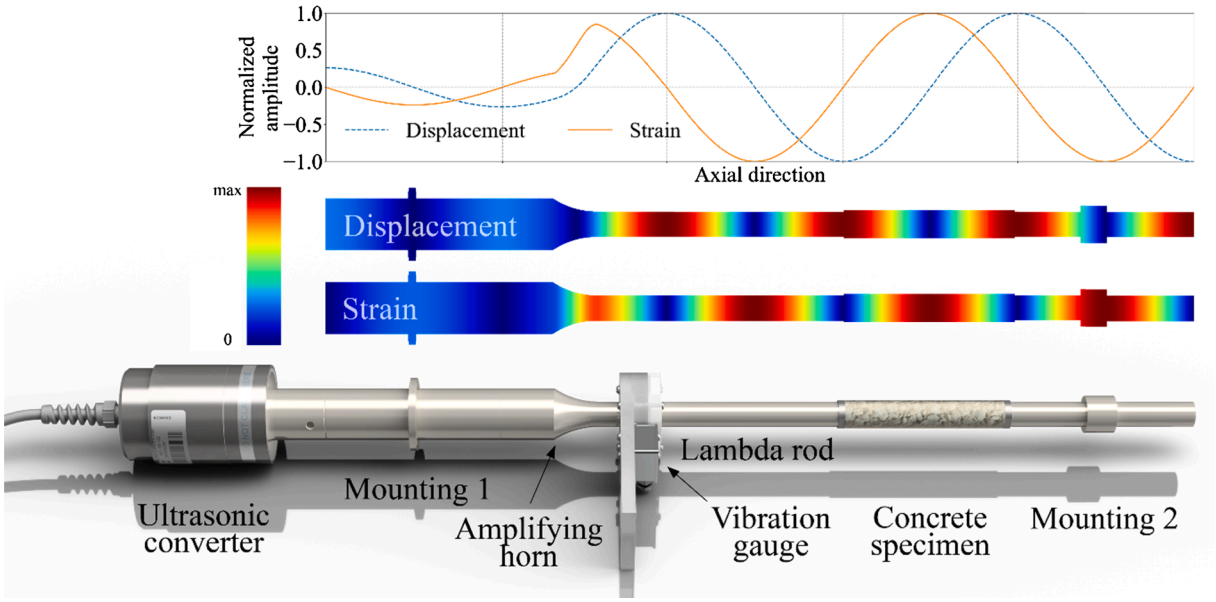

Fig. 1. Schematic representation of the ultrasonic load train for cyclic compression loading with superimposed compression mean loads.

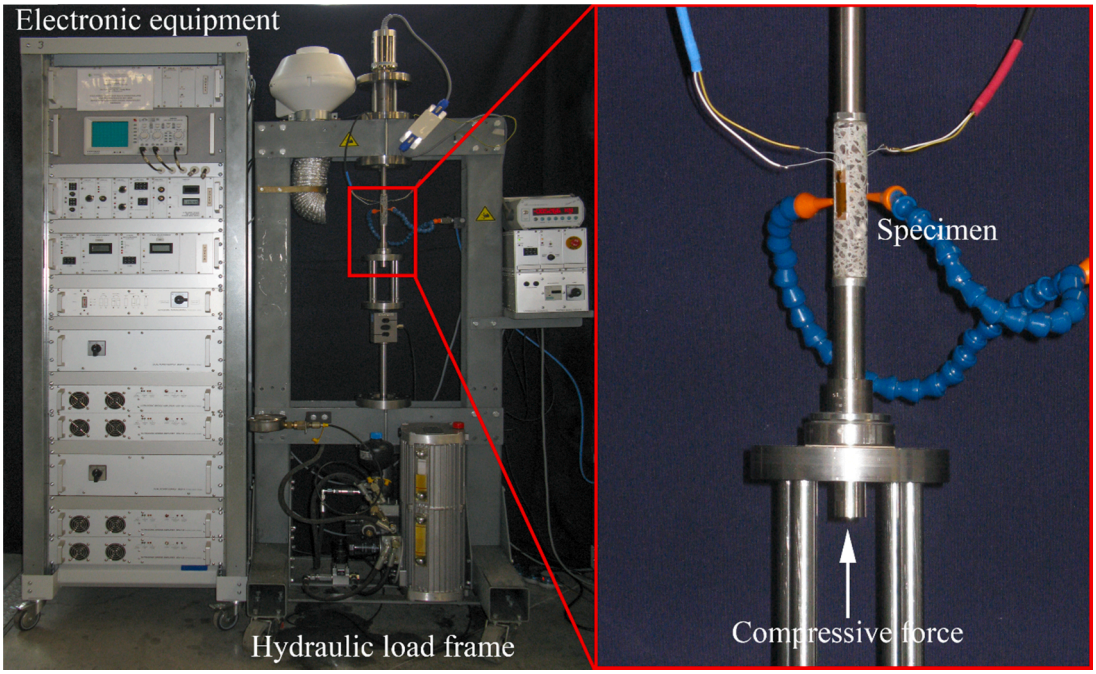

Fig. 2. Setup for ultrasonic fatigue testing of concrete specimens; electronic equipment for test generation and control and hydraulic load frame for generation of static loads (left), detail view at the specimen in the ultrasonic load frame (right).

intermittently in a pulse-pause fashion to avoid undesirable increase of specimen temperature. Pulses of typically 4000 cycles are followed by sufficiently long pauses of 2 s to 8 s. Additional forced-air cooling is employed to keep specimen temperature below an allowable maximum of 40 °C. Due to the intermittent loading, the actual number of cycles applied per second is approximately between 750 and 1800, i.e. the effective cycling frequency is in the 1000 Hz regime, which is still far beyond conventional fatigue testing and accounts for a strong reduction of testing time.

Compressive forces acting as mean loads to the ultrasonic vibration are introduced at two vibration nodes. Forces are generated using a hydraulic load frame (Fig. 2, right) and measured with an S-type load

cell with 20 kN capacity. Accuracy of the applied compressive force is within ± 2 %. Preloads are chosen so that stress remains in the compressive range throughout a load cycle.

Specimens for ultrasonic fatigue testing

Ultrasonic fatigue test specimens are designed to vibrate in resonance, which constrains their overall length to relate to the resonance wavelength. The speed of sound c of a tension–compression (i.e. longitudinal) wave in a straight rod with constant diameter is given by Eq. (1):

$$c = \sqrt{\frac{E}{\rho}} \tag{1}$$

with Young's modulus E and mass density ρ. Wavelength l and vibration frequency f relate to c according to Eq. (2):

$$\lambda \cdot f = c \tag{2}$$

Specimens vibrate at the fundamental resonance frequency, to which the excitation frequency of the ultrasonic system is regulated. Sound waves travelling back and forth in the specimen superimpose to form a standing wave, if the length of the sample follows Eq. (3):

$$l = \frac{\lambda}{2} = \frac{1}{2f}\sqrt{\frac{E}{\rho}} \tag{3}$$

All components of the ultrasonic load train (including the specimen) are designed to resonate close to the converter's resonance frequency of 19 kHz. Given the concrete's mechanical properties stated in Table 1, the resonance length l amounts to 122 mm.

Fig. 3 (left) shows a cylindrical concrete specimen as used in the presented tests. Aluminium discs (with a threaded stub on the top disc) are bonded to the concrete cylinders with epoxy (cured at 40 °C) to ensure good alignment when mounting the specimen into the load train. Additionally, the thin epoxy layer improves sound transfer into the sample. The strain distribution shows a sinusoidal variation along the length of the specimen, with maximum strain amplitude in the centre (i.e. at the vibration node), and zero at its ends. The specimen is loaded with a strain amplitude ≥ 90 % of the nominal amplitude over a length of 35 mm. The output power required to drive the specimen is proportional to the stressed volume, i.e. a larger volume requires higher driving power. The maximum output power of the used testing system is 600 W, which was found to limit the specimen diameter to 21 mm (the length cannot be reduced, to retain resonance length at 19 kHz). The material volume subjected to ≥ 90 % of the nominal amplitude is 12.1 cm^3.

Calibration of ultrasonic fatigue tests

Two strain gauges with a gauge length of 20 mm attached to opposite sides of the centre section of each sample are employed to measure both static and cyclic strains. Stiffness of the samples can be derived from static strain readings that are generated by applying compressive forces with the hydraulic load.

Cyclic ultrasonic fatigue loading occurs displacement controlled. The calibration procedure prior to the fatigue test establishes the linear correlation between the vibration amplitude measured by the induction gauge and the strain amplitude in its centre. Stress can be calculated from the measured strain amplitudes when the stiffness of a sample known. The proportionality between ultrasonic vibration amplitude and stress amplitude is established for each specimen, as stiffness can vary considerably between individual samples. It should be noted that it is not necessary to know the actual value of stiffness since the strain gauges serve as sensors whose sensitivity is determined via applying static compression forces.

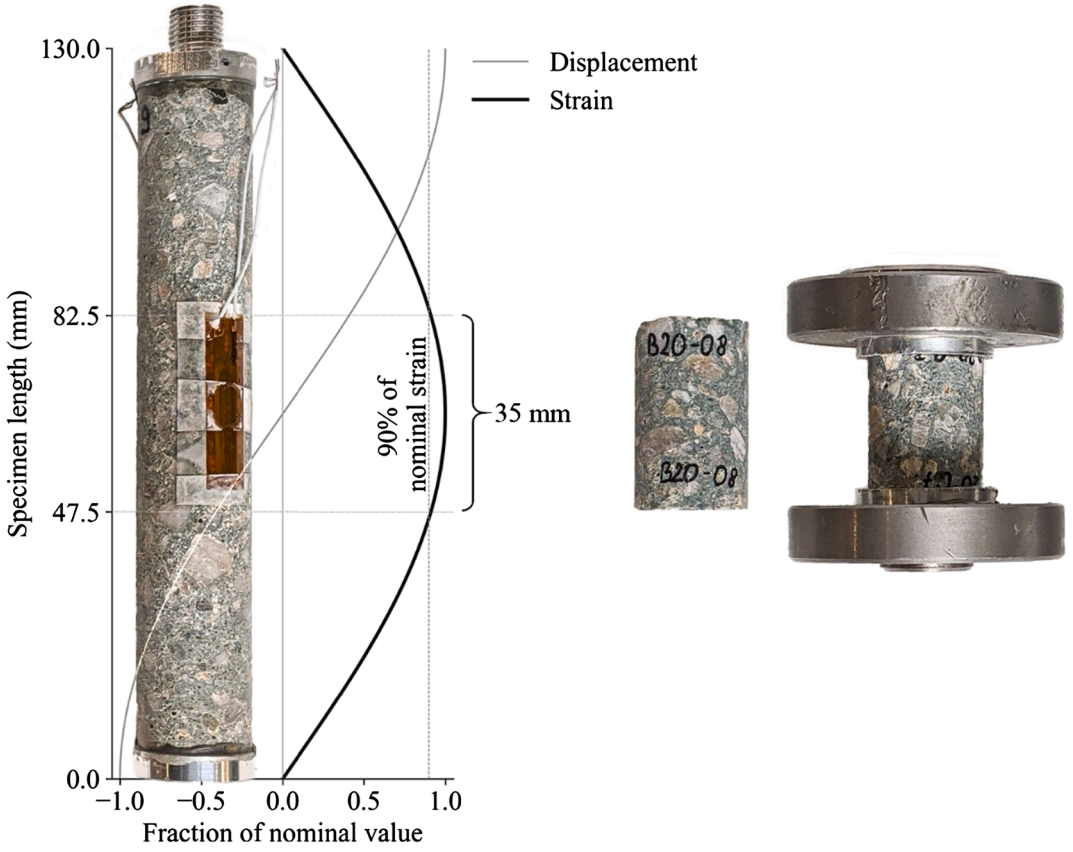

Fig. 3. Specimen geometry used in ultrasonic (left) and in servo-hydraulic tests without attached aluminium rings and pressure plates (right) and mounted ready for testing (far right); the geometry for servo-hydraulic tests is reduced in length (35 mm) to match the testing volume (≥90 % of nominal strain) of the ultrasonic specimens; both geometries have a constant diameter of 21 mm.

Vibration amplitudes and superimposed mean loads are selected so that the sample is cyclically loaded between the minimum compression stress σ_{min} of 5 MPa and the maximum compression stress σ_{max}.

2.2.2. Servo-hydraulic fatigue testing

Servo-hydraulic fatigue tests at have been performed at a cycling frequency of 60 Hz on a 63 kN capacity load frame (Fig. 4) to determine the fatigue properties of the investigated concrete and to serve as reference for the ultrasonic tests. Samples for 60 Hz tests have an overall length of 35 mm. This matches the length over which $\geq$ 90 % of the nominal stress amplitude during ultrasonic loading occurs (Fig. 3). Similar volume stressed in ultrasonic and conventional fatigue tests are used to minimize size effects [26]. Specimens can be cycled continuously in servo-hydraulic tests as specimen heating is negligible.

In contrast to ultrasonic tests, the interfaces between the specimen and the load frame have to bear the nominal cyclic loads during conventional fatigue testing. When the specimens are cut to length from the drill cores the faces end up jagged and less-than-perfectly orthogonal to the length axis to a differing degree, due to individual rock particles debonding from the cement matrix, which would lead to premature failure from the interfaces and excessive scatter of measured lifetimes.

To support the interfaces, the specimens' top and bottom faces are girded in aluminium rings with an inner diameter of 21 mm and a height of 5 mm. The cavities between the rings and the faces are filled with epoxy (cured at 40 °C) and sandwiched between two pressure plates, that are subsequently placed between the load frame's hydraulic piston and load cell. Additionally, an axial bearing is introduced between the top pressure plate and the load cell to counteract bending moments due to insufficient parallelism between the two pressure plates.

3. Results and discussion

3.1. Servo hydraulic fatigue tests

Fatigue lifetimes measured with servo-hydraulic equipment at 60 Hz cycling frequency are shown in Fig. 5. Concrete specimens with a diameter of 21 mm and a length of 35 mm (Fig. 3, right) were cycled sinusoidally between a minimum compression stress, σ_{min}, of 5 MPa and a maximum compression stress, σ_{max}, during a load cycle between 37 % and 75 % of the compressive strength σ_{dB}. IR thermography confirmed that the temperature of specimens cycled in servo-hydraulic tests remained at room temperature during the tests. Failure of the specimens was marked by total obliteration of the concrete cylinders. Specimens

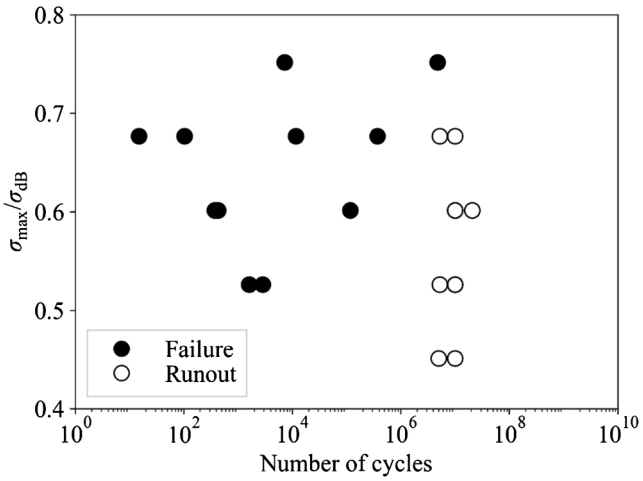

Fig. 5. Lifetime data measured in cyclic compression fatigue tests with servo-hydraulic testing equipment at a cycling frequency of 60 Hz; failed specimens are indicated with solid symbols, specimens that did not fail (runouts) are indicated with open circles; shown on the ordinate is the ratio of the maximum compression stress during a load cycle σ_{max} and the compressive strength σ_{dB} of the tested concrete.

that did not fail within a limiting lifetime of 10^7 cycles were taken off the test and termed runouts.

No failures occurred below 10^7 cycles for cyclic loading with the maximum compression stresses $\leq 0.45\ \sigma_{dB}$. Literature review of fatigue tests with un-notched concrete [12] delivered $0.4 \cdot \sigma_{dB}$ as lower limit for failure within 10^7 cycles, which fits well to the present results. In contrast, both specimens cycled at $0.75 \cdot \sigma_{dB}$ failed below 10^7 cycles. Failures as well as runouts were found at $0.52 \cdot \sigma_{dB}$. Fracture probabilities are calculated by approximating fracture probabilities at different maximum compression stress levels with a Gaussian cumulative probability distribution [28]. With this 50 % fracture probability for a limiting lifetime of 10^7 cycles of $(0.57 \pm 0.06) \cdot \sigma_{dB}$ is found.

It has to be noted that the ultrasonic equipment was originally developed for fatigue testing of metallic materials, where maximum power of 600 W is sufficient. Testing concrete, the maximum power is effectively limiting the stressed volume. For the sake of comparability, the same relatively small stressed volume was used in both, servo-hydraulic and ultrasonic tests. The small stressed volume is a main cause for the observed scatter in fatigue lifetimes, where both the size

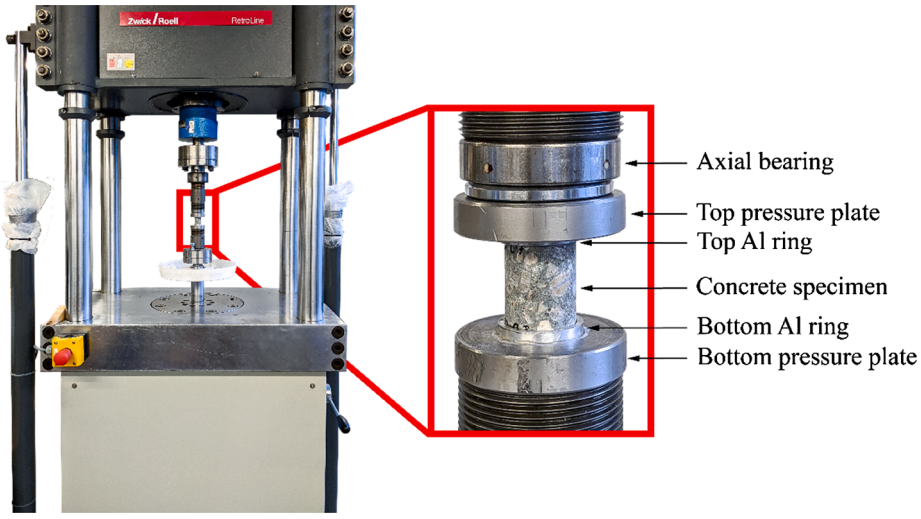

Fig. 4. Setup for servo-hydraulic fatigue testing of concrete specimens with 21 mm diameter; overview of servo-hydraulic load frame (left), and detailed view at the specimen (right).

and the location of single grains have a strong impact on the observed fatigue life of a specimen. This effect is largely smoothed out in standard specimens with approximately two decades larger testing volume.

3.2. Ultrasonic fatigue tests

Fatigue lifetimes measured with both, ultrasonic fatigue testing equipment at 19 kHz cycling frequency, and with servo-hydraulic equipment at 60 Hz cycling frequency are shown in Fig. 6. Specimens in ultrasonic compression fatigue tests (Fig. 3, left) were cycled between a minimum compression stress of 5 MPa and a maximum compression stress during a load cycle between 34 % and 60 % of the compressive strength σ_{dB}, where 0.60 · σ_{dB} was the highest stress that could be realised due to excessive power requirements for cycling the specimen at high amplitudes.

No failures were observed in fatigue tests between 0.34 · σ_{dB} and 0.42 · σ_{dB} within a limiting lifetime of 10^8 cycles. All specimens that were cycled between 0.52 · σ_{dB} and 0.60 · σ_{dB} showed signs of fatigue damage, as will be described below. In servo-hydraulic tests, 3 out of 5 specimens cycled at 0.60 · σ_{dB} failed below 10^7 cycles and 2 out of 4 tested specimens failed at 0.56 · σ_{dB}, respectively. This suggests that fatigue lifetimes and cyclic strength measured in ultrasonic tests are somewhat higher than in servo-hydraulic tests. This would be well in accordance with the frequency influence on fatigue properties of concrete described in the literature [1–3,10,11,13,15].

Criterion for specimen failure

Definition and observation of specimen failure is trivial in conventional or ultrasonic tension–compression or tension–tension fatigue tests, as fatigue lifetime can be specified as the number of cycles until the specimen typically fractures into two halves. This definition for failure is, however, not applicable to ultrasonic cyclic compression testing of concrete, as even with cracks present, the specimen does not disintegrate.

Fatigue damage in concrete is the formation of new and the growth of pre-existing cracks. Cracks increase the compliance and deteriorate the vibration properties of concrete specimens. Since ultrasonic tests are displacement controlled and displacement and strain amplitudes are proportional, strain amplitudes are kept constant during the tests. Stress amplitudes, however, decrease as the compliance of the specimen increases (i.e. stiffness decreases) due to the formation and growth of cracks. Consequently, concrete specimens could not be fractured in the present investigation due to the decrease of cyclic stress, even though fatigue cracks were initiated and propagated. Additional failure criteria aside from specimen rupture into pieces are necessary to specify lifetimes in ultrasonic compression fatigue tests of concrete.

As cracks initiate and grow, however, the power required to drive the specimen increases. As damping of the specimen increases, the time to reach the set amplitude increases (which is counteracted by the closed-loop control). This behaviour is usually employed as one criterion for specimen failure in ultrasonic tests. If the maximum output power cannot drive the vibration amplitude to 85 % the desired level within 100 ms, test generation is halted, and the specimen is considered to have failed. Additionally, a drop in resonance frequency of ≥ 150 Hz from the initial resonance frequency at the beginning of the experiment is another appropriate criterion for failure of a specimen in ultrasonic tests. Both, power and frequency limits are usually used in ultrasonic fatigue tests of metallic specimens to detect failure [24].

The power criterion was fulfilled only for one specimen, that was cycled at 0.6 · σ_{dB} and failed after 2.1 × 10^7 cycles. The conventional criterion of the resonance frequency dropping by 150 Hz was not met by any specimen. However, as detailed below, fatigue damage could also indirectly made visible by fast fourier transformation (FFT) analysis and directly with computed tomography (CT) analysis. With this, the frequency criterion was adapted and a frequency drop of 50 Hz was used as criterion for fracture in the present investigation. Therefore, three different symbols were used to indicate lifetimes in Fig. 6: Specimens that fulfilled the power criterion or the frequency criterion with Δf_{res} = 50 Hz and showed fatigue damage in FFT data and CT are shown with solid red circles. Specimens that fulfilled Δf_{res} = 50 Hz and showed fatigue damage in FFT data and where no CT is available are indicated with hashed red circles. Runouts are indicated with open circles.

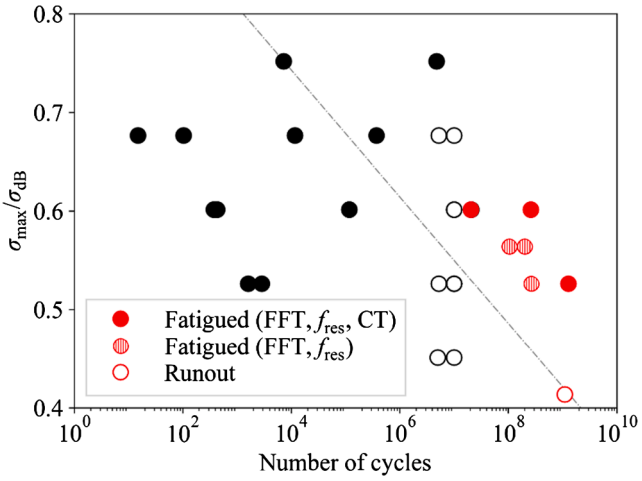

Fig. 6. Lifetime data measured in cyclic compression fatigue tests with ultrasonic testing equipment at a cycling frequency of 19 kHz (red symbols) besides reference data from servo-hydraulic tests from Fig. 5 (black symbols); specimens that showed fatigue damage in FFT data and f_{res} and where damage was confirmed with CT are shown with solid red circles, specimens showing fatigue damage in FFT data and f_{res} and no CT is available are indicated with hashed red circles, runouts are indicated with open circles; lifetimes calculated according to the Model Code 2010 [18] for σ_{min} = 5 MPa are indicated with a dash-dotted line.

3.3. Monitoring of fatigue damage in ultrasonic tests

Several methods have been developed in different ultrasonic fatigue testing applications to monitor the progress of fatigue damage. However, these techniques have been originally developed for testing metallic materials under cyclic tension–compression or cyclic tension loading: The decrease of cycling frequency has been used to detect crack initiation and specimen failure already in older ultrasonic literature [29]. Measurement of temperature increase during ultrasonic cycling has been used to indirectly calculate the cyclic plastic deformation during a load cycle [30]. Non-destructive evaluation of material damage is possible with acoustic methods, in which sound waves travelling through a material volume are analysed for echoes and harmonic features [31,32]. More recently, the evaluation of vibration properties and real-time signal processing was established to monitor the progress of fatigue damage in cast aluminium [33] and nickel-based superalloys [34]. These methods are adapted in the present work and used to monitor the progress of fatigue damage in concrete specimens subjected to ultrasonic compression loading.

Specimen surface temperature

Thermographic measurements of specimen surface temperature have been performed to make the heat generation caused by irreversible cyclic deformation visible. The experiments are performed with an InfraTec VarioCAM IR at a rate of 60 frames per second, which allows to capture the surface temperature increase over single ultrasonic pulses.

The measurements are used to quantify heat generation and variation of temperature across the specimen surface. The following measurement procedure is applied: Initially, the specimen is cycled in a pulse-pause sequence until a steady state condition of the temperature is reached. Then, the specimen is loaded with one pulse of 100 ms duration (approx. 1900 load cycles), while the temperature increase is monitored simultaneously. Due to the short pulse length and the

relatively small temperature increases during the pulse ($\lessapprox 1$ °C), the heat loss due to convection is assumed to be negligible, as is heat transport due to thermal conduction during the ultrasonic pulse.

Cycling a concrete sample at ultrasonic frequency causes an increase of its temperature due to the heat produced by irreversible deformation. Deviation from the linear elastic behaviour due to irreversible deformation leads to a hysteresis loop between stress and strain, the area of which is proportional to the dissipated heat during cycling. Therefore, the heat produced per cycle can be used to estimate the irreversible strain amplitude.

Specimen surface temperature versus time during one ultrasonic pulse of 100 ms duration is shown in Fig. 7. The temperature distribution over the specimen surface at the end of the pulse is shown to the left. It shows an inhomogeneous distribution of ΔT, which suggests a varying irreversible deformation with localized damage across the specimen surface. To the right, surface temperature averaged over the central region of interest versus time is shown. The temperature increases linearly during the pulse. After the end of the pulse, it decreases again slowly. The maximum temperature increase is about 0.71 °C at the end of the pulse with maximum compression stress *of* $0.53 \cdot \sigma_{dB}$, and 0.87 °C for $\sigma_{max} = 0.60 \cdot \sigma_{dB}$, respectively.

The temperature increases during an ultrasonic pulse can be used to approximately calculate the irreversible strain amplitude. Cyclic loading causes reversible as well as irreversible deformation. For the calculation of the irreversible strain a certain shape of the stress–strain curve must be assumed. A method previously used for the determination of plastic strain amplitude in metals during ultrasonic cycling [30] is to assume an elliptical shape of the stress–strain curve with the elastic strain amplitude ε_{el} being half of the major axis, and the irreversible strain amplitude ε_{irr} being half of the minor axis of the ellipse, respectively. Nearly linear elastic behaviour is assumed, i.e. the elastic strain amplitude approximately follows the stress amplitude σ_a according to Hooke's law. The generated heat ΔQ in the material volume ΔV over the course of a single load cycle is given by Eq. (4):

$$\Delta Q = \Delta V \cdot \pi \cdot \sigma_a \cdot \varepsilon_{irr} \tag{4}$$

This causes an increase of specimen temperature. With the specific heat of the material c and its mass density ρ, the temperature increases by ΔT over the course of ΔN load cycles. The heat generated over the course of a single load cycle can be written as Eq. (5):

$$\Delta Q = \rho \cdot \Delta V \cdot c \cdot \frac{\Delta T}{\Delta N} \tag{5}$$

This leads to Eq. (6) for the irreversible strain amplitude:

$$\varepsilon_{irr} = \frac{\rho \cdot c \cdot \Delta T / \Delta N}{\pi \cdot \sigma_a} \tag{6}$$

The temperature increase during an ultrasonic pulse can be seen in Fig. 7. Analysing the data, $\Delta T/\Delta N$ is approximately 3.7×10^{-4} K for cycling with a maximum compression stress of $0.53 \cdot \sigma_{dB}$, and 4.8×10^{-4} K for cycling with $\sigma_{max} = 0.60 \cdot \sigma_{dB}$. Assuming a specific heat of 1 kJ/kgK and a mass density of 2.4 g/cm^3, the irreversible strain amplitudes are 9×10^{-6} ($0.53 \cdot \sigma_{dB}$), and 10^{-5} ($0.60 \cdot \sigma_{dB}$), respectively, amounting to about 1 % of the elastic strain amplitude.

These irreversible strain amplitudes are calculated for ultrasonic frequency loading. Strain rates in the ultrasonic frequency tests are in the in the order of 10^1 s^{-1}, whereas they are about a factor 1000 lower in servo-hydraulic tests. According to the data compiled in [25], this increase of strain rate increases the compressive strength of concrete by about 20 %. Due to the higher static strength at the high strain rate, the irreversible strain calculated for ultrasonic frequency cycling will be higher than for conventional frequency cycling.

Power for maintaining vibration amplitude

With Eq. (5) the ultrasonic power output P required to drive the experiment can be derived according to Eq. (7):

$$P = \frac{\Delta Q}{\Delta t} = \frac{\rho \cdot \Delta V \cdot c \cdot \Delta T / \Delta N}{\Delta t} \tag{7}$$

The timestep Δt is 53 µs, the duration of one ultrasonic cycle at 19 kHz. With this, $P = 260$ W for the experiment with $\sigma_{max} = 0.60 \cdot \sigma_{dB}$. Irreversible deformation in the specimen consumes most of the ultrasonic power, and little power is undesirably lost in the load train, which points to the suitability of the used ultrasonic load train. The ultrasonic fatigue testing equipment has a maximum effective power output of 600 W under optimum conditions (i.e. perfect matching of the ultrasonic power signal, minimum power loss due to internal friction in components of the load train other than the concrete specimen, and across interfaces). However, active control of ultrasonic vibration requires additional headroom to maintain a constant vibration amplitude. Initiation of cracks during the fatigue tests deteriorate the vibration properties of the specimens and increases the power requirements. Thus, the maximum continuous power available for ultrasonic tests should be maximum half of the maximum power output of the ultrasonic equipment to allow control of vibration amplitude during the experiment.

Ultrasonic transducers as well as ultrasonic amplifiers with maximum power ratings of 4000 W are available commercially. It should therefore be feasible to develop an ultrasonic fatigue testing setup with approximately a factor 6.7 more power than the setup presently used. The diameter of a specimen therefore could be a factor of 2.6

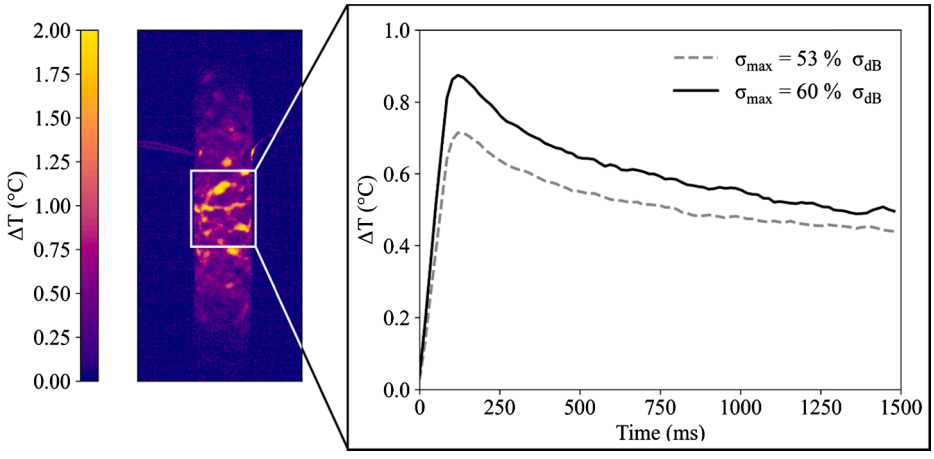

Fig. 7. Surface temperature response of a concrete specimen subjected to ultrasonic cycling; temperature increase relative to the steady state approximately 200 ms after the onset of an ultrasonic pulse of 100 ms length, followed by a pause of 8000 ms (left), temporal evolution of surface temperature averaged over the gauge section for $\sigma_{max} = 0.60 \cdot \sigma_{dB}$ and $0.53 \cdot \sigma_{dB}$, respectively (right).

larger, i.e. specimens with diameter 54 mm seem possible. The length of the specimen, however, cannot be changed since it must meet resonance condition.

Resonance frequency

An increase in number and length of fatigue cracks in the concrete specimens leads to changes of their resonance vibration properties, such as, an increase of compliance, an increase of damping resulting in an increase of power necessary to drive the vibration, and the generation of higher order harmonics of the soundwave traveling through the specimen across numerous (newly formed) interfaces and defects. These changes of physical properties can be detected, quantitatively determined and used as a measure for the progress of fatigue damage in the concrete specimen as described in the following:

The resonance frequency of the load train is used as a measure for the specimen's compliance. As compliance increases, the resonance frequency of the specimen and thus the resonance frequency of the entire resonating load train decreases. By monitoring the resonance frequency and comparing it to the initial resonance frequency with the virgin specimen mounted in the load train, the evolution of fatigue damage can be visualized.

The course of resonance frequency f_{res} versus number of cycles N is shown in Fig. 8 (top) for a specimen that was cycles at a maximum compression stress of $0.60 \cdot \sigma_{dB}$. It can be seen that, after a steep initial drop in resonance frequency that is attributed to warming up of the ultrasonic load train, f_{res} monotonously decreased over the course of the experiment, indicating the initiation of new and growth of existing cracks, even though the specimen did not fail (according to the power criterion) until the test was stopped at 2.6×10^8 load cycles after f_{res} had dropped by 50 Hz from steady state.

It has been mentioned earlier that no specimen showed failure following the "conventional" frequency criterion (i.e. $\Delta f_{res} = 150$ Hz). This results from the decreasing cyclic stress with increasing compliance, limiting the length of fatigue cracks and thus the observed drop in resonance frequency. It will be shown later that specimens that showed a drop of 50 Hz that were investigated in computed tomography (CT) scans exhibit significant fatigue damage. Consequently, all specimens that showed a drop in resonance frequency of 50 Hz are termed failures and are marked accordingly in Fig. 6.

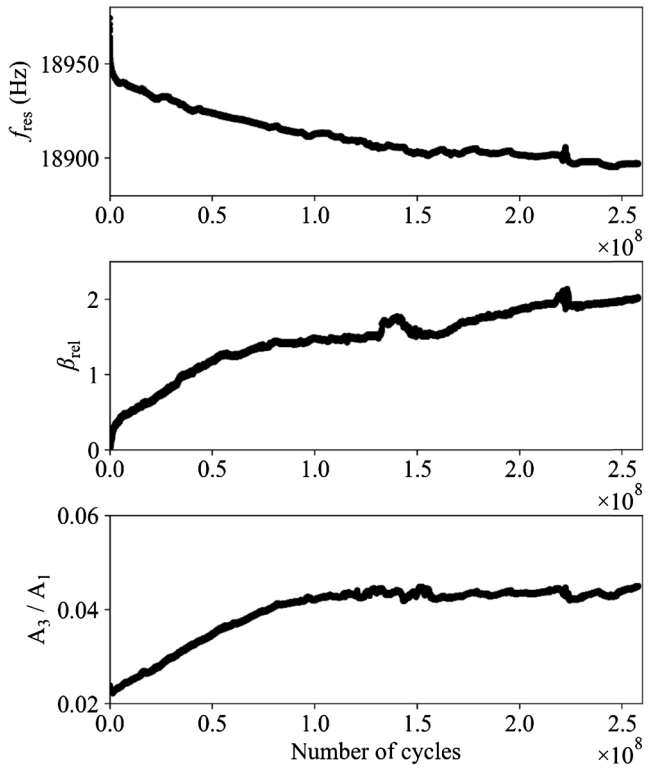

Fig. 8. Specimen vibration properties versus number of cycles for a specimen cycled with $\sigma_{max} = 0.6 \cdot \sigma_{dB}$; resonance frequency (top), non–linearity parameter β_{rel} [33,34] (middle), and amplitude ratio of third harmonic overtone A_3 (at approx. 59 kHz) to fundamental frequency A_1 (bottom).

Non-linearity of vibration

Fatigue cracks cause damping and reflexions of sound waves that are travelling through the specimen. As a consequence, second and higher order harmonics of the fundamental sound wave are generated. Nonlinear propagation behaviour of ultrasonic waves can be exploited in order to assess fatigue damage in progress [33,34]. The displacement signal from the vibration gauge is analysed in a Fast Fourier Transform algorithm for extracting the amplitude and frequency of the fundamental vibration and its harmonic overtones [35]. The nonlinearity parameter β is derived from the amplitude of the fundamental vibration (A_1), the amplitude of the second order harmonic at around 38 kHz (A_2) and the length of the specimen:

$$\beta = \frac{A_2}{A_1^2} \cdot \frac{4l}{\pi^2} \tag{8}$$

Vibration properties of virgin samples may differ between specimens. Moreover, the load train itself contains a certain harmonic overtone content, e.g. interfaces between components also introduce nonlinearity into the feedback signal. Therefore, the relative change of the non-linearity parameter rather than its absolute value is evaluated. The relative non-linearity parameter β_{rel} is the ratio of the current nonlinearity parameter β, measured continuously during the experiment and the non-linearity parameter β_0 measured at the beginning of the experiment for the virgin specimen:

$$\beta_{rel} = \frac{\beta}{\beta_0} \tag{9}$$

Observation of the relative non-linearity parameter is a third method to in-situ monitor the progress of fatigue damage in the concrete specimens. However, the parameter was not used as failure criterion in the present work, as the data basis for assessing absolute values of β_{rel} is too scarce and more experience and knowledge about the vibration properties of the material under investigation are required to interpret the non-linearity parameter correctly.

The presented tests are among the first ultrasonic fatigue tests of concrete, and specifically under cyclic compression loading. Consequently, the time series of β_{rel} versus number of cycles shown in Fig. 8 (middle) are only interpreted qualitatively. Studies available in the literature using this method have been investigating metallic materials only [33–38]. It can be seen that the course of the β_{rel} is inverse to f_{res} (Fig. 8, top). The amplitude A_1 of the fundamental vibration is virtually constant throughout the test, as it is the process variable that is kept constant by the closed-loop control amplitude. The monotonous increase of β_{rel} therefore results from an increase in A_2, which is expected as new cracks initiate, existing cracks grow, and new interfaces and material discontinuities are formed.

A conceptually very similar analysis shown in Fig. 8 (bottom) is the ratio of A_3/A_1 versus number of cycles N. Again, A_1 is constant and the increase in the ratio is due to the increasing amplitude A_3 of the third harmonic overtone at around 57 kHz. As the initially (ideally) purely sinusoidal feedback signal deteriorates with increasing N, the generation of odd harmonic overtones is increasingly promoted.

Together, f_{res}, β_{rel} and A_3/A_1 indicate that already early into the experiment, fatigue damage is detected, even if the ultrasonic equipment did not stop due to power or frequency limits within the limiting lifetime. Analysing the vibration properties, fatigue damage could be detected in three specimens cycled between $0.53 \cdot \sigma_{dB}$ and $0.60 \cdot \sigma_{dB}$, that did not fail, with both, β_{rel} and A_3/A_1 showing absolute values very similar to the specimen that failed at $0.60 \cdot \sigma_{dB}$, which is marked accordingly in Fig. 6.

CT scans

Computed tomography (CT) scans of several ultrasonic fatigue specimens were acquired before and after cyclic loading with a GE Phoenix v|tome|x m 300 in 21 layers with an equidistant spacing of 1.5 mm along the central 30 mm of the specimen's length, to identify fatigue damage especially in runout specimens (e.g. cracks in cement matrix, aggregates, or interfaces between matrix and aggregates). Two CT cross-sections taken from a runout specimen before and after ultrasonic loading for 2.6×10^8 cycles at $\sigma_{max} = 0.6 \cdot \sigma_{dB}$ are shown in Fig. 9 (the same specimen as in Fig. 8). In the first cross-section (top-row) in can be seen that a grain in sector 14 has fractured, as well as debonded from the matrix. In the second cross-section (bottom row), a crack has emanated from a pore in section 8 and grown into the matrix, extending into sector 16. Similar evidence of fatigue damage has been found in other runout specimens, suggesting that, even though the ultrasonic equipment did not stop due to power or frequency limits, fatigue damage in ultrasonic fatigue tests did occur in these specimens.

Comparing CT scans before and after cyclic loading, fatigue damage could be detected in specimens that were cycled between $0.53 \cdot \sigma_{dB}$ and $0.60 \cdot \sigma_{dB}$, which is marked accordingly in Fig. 6.

4. Conclusions

The ultrasonic fatigue testing method is used to study the cyclic compression fatigue properties of concrete at a cycling frequency of 19 kHz. S–N data measured at 60 Hz with servo-hydraulic equipment served for comparison. The following conclusions may be drawn:

1. It is in principle possible to study the very high cycle fatigue (VHCF) properties of concrete under cyclic compression loading with the ultrasonic fatigue testing method. This leads to a vast acceleration of tests and allows investigations in the VHCF regime (i.e. regime of load cycles above 10^7) within reasonable testing times.

2. Specimens disintegrate in stress controlled servo-hydraulic tests. Therefore, the lifetime resulting from a servo-hydraulic test is trivially defined. Ultrasonic tests are displacement controlled. Specimens still accumulate fatigue damage but do not disintegrate. The introduction of fatigue cracks increases the specimen compliance. Keeping the displacement amplitude constant leads to a reduction of the cyclic load. Thus, fatigue cracks can be initiated but the specimen cannot be ruptured in ultrasonic tests.

3. Due to decreasing cyclic stress with increasing specimen compliance, longer lifetimes are measured with the displacement controlled ultrasonic fatigue testing method. Also, increasing compressive strength of concrete with increasing strain rate is reported in the literature, which increases measured lifetimes compared to servo-hydraulic tests.

4. Several criteria are successfully applied to characterize fatigue damage in the ultrasonic experiment: The resonance frequency

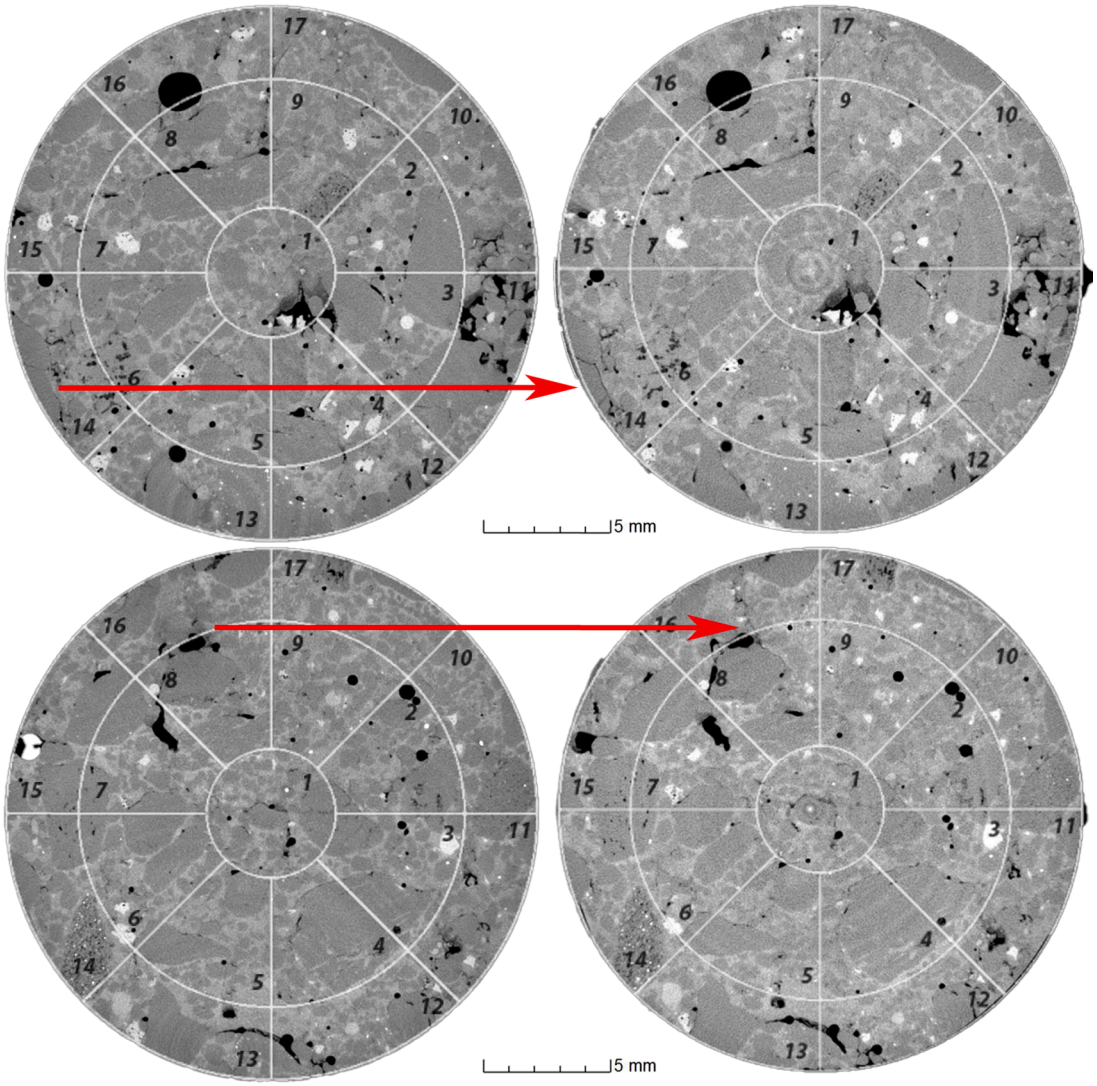

Fig. 9. CT cross-sections taken from the sample shown in Fig. 8; 10.5 mm above the specimen center (top row) and 9.0 mm above, respectively (bottom row), before loading (left column) and after cyclic loading at $\sigma_{max} = 0.6 \cdot \sigma_{dB}$ for 2.6×10^8 cycles (right column); red arrows indicate locations showing fatigue damage.

decreases due to the initiation of fatigue cracks. Analysis of vibration properties and evaluation of first and second order harmonic can indicate fatigue damage. Computed tomography of virgin specimens and after ultrasonic fatigue loading make fatigue cracks produced during the experiment visible.

5. Measurement of temperature in ultrasonic tests can be used to calculate the cyclic irreversible strain, which is about 1 % of the elastic strain amplitude for VHCF failure. Irreversible deformation in the specimen consumes most of the ultrasonic power, and little power is undesirably lost in the load train, which points to the suitability of the used ultrasonic load train. The ultrasonic power necessary to drive the experiment limited the diameter of the concrete specimen in the present tests. However, moving to (significantly) larger specimen diameter should be feasible by adapting commercially available ultrasonic equipment with more power.

6. For future investigations, a common metric for direct comparison of lifetime between conventional stress controlled and ultrasonic displacement controlled fatigue data should be developed. This could be based on monitoring specimen stiffness over the course of the experiments. At the same time, raising the maximum output power of the ultrasonic fatigue testing system could enable the investigation of larger stressed volumes, thus reducing scatter of lifetimes and improving comparability between conventional and ultrasonic tests.

CRediT authorship contribution statement

Michael Fitzka: Methodology, Formal analysis, Validation, Investigation, Resources, Data curation, Writing - original draft, Visualization, Project administration. **Ulrike Karr:** Methodology, Formal analysis, Investigation, Resources, Data curation, Visualization. **Maximilian Granzner:** Formal analysis. **Tomáš Melichar:** Investigation, Resources. **Martin Rödhammer:** Investigation, Project administration, Funding acquisition. **Alfred Strauss:** Resources, Supervision. **Herwig Mayer:** Conceptualization, Methodology, Validation, Formal analysis, Writing - original draft, Supervision, Project administration, Funding acquisition.

Declaration of Competing Interest

The authors declare that they have no known competing financial interests or personal relationships that could have appeared to influence the work reported in this paper.

Acknowledgements

The authors thank Benjamin Täubling–Fruleux for preparing concrete cylinders and Rostislav Drochytka for help performing the CT scans.

References

[1] P.R. Sparks, J.B. Menzies, The effect of rate of loading upon the static and fatigue strengths of plain concrete in compression, Mag. Concr. Res. 25 (1973) 73–80.
[2] H. Reinhardt, P. Stroeven, J. Den Uijl, T. Kooistra, J. Vrencken, Einfluss von Schwingbreite, Belastungshöhe und Frequenz auf die Schwingfestigkeit von Beton bei niedrigen Bruchlastwechselzahlen, Betonwerk und Fertigteil-Technik 44 (1978) 498–503.
[3] B. Zhang, D.V. Phillips, K. Wu, Effects of loading frequency and stress reversal on fatigue life of plain concrete, Mag. Concr. Res. 48 (1996) 361–375.
[4] J.-K. Kim, Y.-Y. Kim, Experimental study of the fatigue behavior of high strength concrete, Cem. Concr. Res. 26 (1996) 1513–1523.
[5] M. Schläfli, E. Brühwiler, Fatigue of existing reinforced concrete bridge deck slabs, Eng. Struct. 20 (1998) 991–998.
[6] M.K. Lee, B.I.G. Barr, An overview of the fatigue behaviour of plain and fibre reinforced concrete, Cem. Concr. Compos. 26 (2004) 299–305.
[7] B. Mu, K.V. Subramaniam, S.P. Shah, Failure Mechanism of Concrete under Fatigue Compressive Load, J. Mater. Civ. Eng. 16 (2004) 566–572.
[8] R. Harte, G.P.A.G. Van Zijl, Structural stability of concrete wind turbines and solar chimney towers exposed to dynamic wind action, J. Wind Eng. Ind. Aerodyn. 95 (2007) 1079–1096.
[9] C. Zanuy, L. Albajar, P. De la Fuente, The fatigue process of concrete and its structural influence, Materiales de Construcción 61 (2010) 385–399.
[10] S. Schneider, D. Vöcker, S. Marx, Zum Einfluss der Belastungsfrequenz und der Spannungsgeschwindigkeit auf die Ermüdungsfestigkeit von Beton, Beton-Stahlbetonbau 107 (2012) 836–845.
[11] L. Saucedo, R.C. Yu, A. Medeiros, X. Zhang, G. Ruiz, A probabilistic fatigue model based on the initial distribution to consider frequency effect in plain and fiber reinforced concrete, Int. J. Fatigue 48 (2013) 308–318.
[12] L. Susmel, A unifying methodology to design un-notched plain and short-fibre/particle reinforced concretes against fatigue, Int. J. Fatigue 61 (2014) 226–243.
[13] A. Medeiros, X. Zhang, G. Ruiz, R.C. Yu, M.d.S.L. Velasco, Effect of the loading frequency on the compressive fatigue behavior of plain and fiber reinforced concrete, International Journal of Fatigue, 70 (2015) 342-350.
[14] C. von der Haar, S. Marx, Development of stiffness and ultrasonic pulse velocity of fatigue loaded concrete, Structural Concrete 17 (2016) 630–636.
[15] J. Hümme, C. von der Haar, L. Lohaus, S. Marx, Fatigue behaviour of a normal-strength concrete – number of cycles to failure and strain development, Structural Concrete 17 (2016) 637–645.
[16] O. Jadallah, C. Bagni, H. Askes, L. Susmel, Microstructural length scale parameters to model the high-cycle fatigue behaviour of notched plain concrete, Int. J. Fatigue 82 (2016) 708–720.
[17] T. Scheiden, N. Oneschkow, Influence of coarse aggregate type on the damage mechanism in high-strength concrete under compressive fatigue loading, Structural Concrete 20 (2019) 1212–1219.
[18] fib, fib Model Code for Concrete Structures 2010, (2013).
[19] Y. Zhang, W. Zhang, W. She, L. Ma, W. Zhu, Ultrasound monitoring of setting and hardening process of ultra-high performance cementitious materials, NDT and E Int. 47 (2012) 177–184.
[20] S. Liu, J. Zhu, S. Seraj, R. Cano, M. Juenger, Monitoring setting and hardening process of mortar and concrete using ultrasonic shear waves, Constr. Build. Mater. 72 (2014) 248–255.
[21] L.E. Willertz, Ultrasonic Fatigue, Int. Metall. Rev. 2 (1980) 65–78.
[22] L.D. Roth, Ultrasonic Fatigue Testing, in: J.R. Newby, J.R. Davis, S.K. Refsnes, D. A. Dietrich (Eds.), ASM Handbook, ASTM, Philadelphia, 1992, pp. 240–258.
[23] H. Mayer, Fatigue crack growth and threshold measurements at very high frequencies, Int. Mater. Rev. 44 (1999) 1–36.
[24] H. Mayer, Recent developments in ultrasonic fatigue, Fatigue Fract. Eng. Mater. Struct. 39 (2016) 3–29.
[25] P.H. Bischoff, S.H. Perry, Compressive behaviour of concrete at high strain rates, Mater Struct 24 (1991) 425–450.
[26] Z.P. Bazant, J. Planas, Fracture and Size Effect in Concrete and Other Quasibrittle Materials, Taylor & Francis, 1997.
[27] U. Karr, R. Schuller, M. Fitzka, A. Denk, A. Strauss, H. Mayer, Very high cycle fatigue testing of concrete using ultrasonic cycling, Materials Testing 59 (2017) 438–444.
[28] W.W. Maenning, Planning and evaluation of fatigue tests, in: S.R. Lampman, G.M. Davidson, F. Reidenbach, R.L. Boring, A. Hammel, S.D. Henry, W.W.S. jr (Eds.) ASM Handbook Fatigue and Fracture, ASM International, Materials Park OH, 1997, pp. 303-313.
[29] S.E. Stanzl, Fatigue Testing at Ultrasonic Frequencies, J. Soc. of Environm. Engineers 25–1 (1986) 11–16.
[30] M. Papakyriacou, H. Mayer, H. Plenk, S. Tschegg, Cyclic plastic deformation of tantalum and niobium at very high numbers of cycles, Mater. Sci. Engng., A 325 (2002) 520–524.
[31] M. Hong, Z. Su, Q. Wang, L. Cheng, X. Qing, Modeling nonlinearities of ultrasonic waves for fatigue damage characterization: theory, simulation, and experimental validation, Ultrasonics 54 (2014) 770–778.
[32] Z. Su, C. Zhou, M. Hong, L. Cheng, Q. Wang, X. Qing, Acousto-ultrasonics-based fatigue damage characterization: Linear versus nonlinear signal features, Mech. Syst. Sig. Process. 45 (2014) 225–239.
[33] A. Kumar, C. Torbet, T. Pollock, J.W. Jones, In situ characterization of fatigue damage evolution in a cast Al alloy via nonlinear ultrasonic measurements, Acta Mater. 58 (2010) 2143–2154.
[34] A. Kumar, C.J. Torbet, J.W. Jones, T. Pollock, Nonlinear ultrasonics for in situ damage detection during high frequency fatigue, J Appl Phys 106 (2009) 0249011–0249019.
[35] H. Mayer, M. Fitzka, R. Schuller, Constant and Variable Amplitude Ultrasonic Fatigue of 2024–T351 Aluminium Alloy at Different Load Ratios, Ultrasonics 53 (2013) 1425–1432.
[36] T. Kirsten, F. Bülbül, T. Stein, M. Wicke, H.-J. Christ, A. Brückner-Foit, M. Zimmermann, Characterization of crack initiation and crack growth in the VHCF regime on the basis of nonlinear material behaviour in comparison to optical investigations for two aluminum alloys, in: M. Zimmermann, H.-J. Christ (Eds.), VHCF7, Universität Siegen, Dresden, Germany, 2017.
[37] D. Krewerth, T. Lippmann, A. Weidner, H. Biermann, Application of full-surface view in situ thermography measurements during ultrasonic fatigue of cast steel G42CrMo4, Int. J. Fatigue 80 (2015) 459–467.
[38] M. Seleznev, A. Weidner, H. Biermann, A. Vinogradov, Novel method for in situ damage monitoring during ultrasonic fatigue testing by the advanced acoustic emission technique, Int. J. Fatigue 142 (2021), 105918.